

# Scanning-tunneling-microscopy images of oxygen adsorption on the Si(001) surface

Toshihiro Uchiyama

*Matsushita Research Institute Tokyo, Inc., 3-10-1 Higashi-mita, Tama-ku, Kawasaki 214, Japan*

Masaru Tsukada

*Department of Physics, University of Tokyo, 7-3-1 Hongo, Bunkyo-ku, Tokyo 113, Japan*

(Received 4 October 1996; revised manuscript received 27 November 1996)

We investigate the atomic structures and scanning-tunneling-microscopy (STM) images of oxygen adsorption on the Si(001) surface. Here, three (meta)stable sites for atomic adsorption are discussed: a backbond of down dimer atom, a dimer-bridge, and an on-dimer site. For this study, the first-principles molecular-dynamics method incorporating the ultrasoft pseudopotential scheme is applied. The oxygen gives a surface structure characteristic of the adsorption site. In particular, the Si-O-Si complex at the dimer-bridge site buckles so as to mimic the original dimer. In the filled states, the STM images for the backbond and the dimer-bridge site appear very similar. In contrast, the empty-states images show characteristic features of the oxygen site. [S0163-1829(97)05515-X]

## I. INTRODUCTION

Oxidation of silicon surfaces has attracted much attention because of its scientific interest and technological importance. For this reason, a number of works have been devoted to revealing atomic structures of oxide complexes at submonolayer coverage. On the Si(001) surface, some different sites of oxygen adsorption have been proposed experimentally: dimer-bridge,<sup>1,2</sup> backbond,<sup>1,3-5</sup> and on-top sites.<sup>6</sup> Recently, scanning tunneling microscopy (STM) has been extensively applied for these studies.<sup>5,7-9</sup> For example, Kliese *et al.*<sup>7</sup> have found small protrusions of about 0.2 Å height at the very early stage of the oxidation. Around these spots, local dimer buckling seems to be stabilized. By utilizing scanning tunneling spectroscopy (STS), Ikegami *et al.*<sup>5</sup> have revealed that oxygen lies even in the seemingly 2×1 surface of the image. They have insisted on the adsorption at a backbond site.

In the first-principles total-energy and force calculations,<sup>10-12</sup> a few (meta)stable adsorption sites are obtained, corresponding to the experimental findings. In Ref. 12, we have simulated the STM images of the adsorption on the Si(001) surface, even though any sites with the predicted features have not yet been identified in the STM observations. In the previous calculations, however, we are restricted to the unit cell of  $p(2 \times 1)$  with a single oxygen atom inside. The coverage of a half monolayer might be inadequately large to describe the oxides at the initial stage. In this study, the unit cell is extended to  $p(2 \times 2)$  in order to incorporate surface relaxation more properly. Then, we reinvestigate the atomic geometries and STM images of the adsorption. Here, a backbond (BBD) of the down atom, a dimer-bridge (DB), and an on-dimer (OD) site are discussed, because of their energetic stability.

In the following, we apply the first-principles molecular-dynamics method.<sup>13,14</sup> It is based on the local density functional formalism with the ultrasoft pseudopotential scheme of Vanderbilt.<sup>15</sup> The details of our method are summarized in Ref. 12. The cutoff energy is set to be  $E_{\text{cut}} = 25$  Ry. For the

Si(001) surface, we adopt a repeated slab model consisting of eight atomic layers of Si and a vacuum gap with an appropriate thickness. With an oxygen atom on each side of the slab, we optimize the atomic geometry until the residual forces acting on each atom are less than  $5 \times 10^{-3}$  Ry/a.u. Furthermore, the tunneling current of the STM,  $I(\mathbf{r}, V_S)$ , is simply approximated as

$$I(\mathbf{r}, V_S) \propto \pm \int_{E_F}^{E_F + eV_S} dE \rho(\mathbf{r}, E), \quad (1)$$

where the plus (minus) sign is for the positive (negative) surface bias voltage  $V_S$ . Here,  $\rho(\mathbf{r}, E)$  is the local density of states at energy  $E$ , and  $E_F$  is the Fermi energy.

## II. ATOMIC STRUCTURES AND STM IMAGES

First, we determine the asymmetric dimer geometry of the Si(001) surface. The bond length is  $d = 2.32$  Å and the buckling angle  $\phi = 17.7^\circ$  on the average as in Table I. A perspective view of the surface is shown in Fig. 1(a). These values agree fairly well with the recent results of the first-principles calculations by Ramstad, Brocks, and Kelly<sup>16</sup> and Fritsch and Pavone,<sup>17</sup>  $d = 2.28$  Å and  $\phi = 19.1^\circ$ , and  $d = 2.33$  Å and  $\phi = 18.5^\circ$ , respectively.

Next, we adsorb an oxygen atom onto the surface. Perspective views of the optimized structures for the BBD, the DB, and the OD site are shown in Figs. 1(b)–1(d), respectively. The reacted dimer twists, breaks up, or gets almost symmetric. The Si—O bond lengths  $d_{\text{Si—O}}$  and the bond angle of the oxygen  $\theta_{\text{Si—O—Si}}$  are tabulated in Table I. Those agree well with the values of crystalline silica<sup>18</sup> of 1.52–1.69 Å and 137–180°, except the angle at the OD site. The bond length  $d_i$  and the tilting  $\phi_i$  of the Si dimers are also given in the table. The suffix  $i=1$  ( $i=2$ ) indicates the reacted (unreacted) dimer. Here, the tilting  $\phi_i$  is defined as the angle between the bond and the [110] direction. The bond angles around the up (down) atom are summed to  $\xi_{iu}$  ( $\xi_{id}$ ) in the table. The angles for the OD site are formed by the Si—O

TABLE I. Geometrical parameters of the oxygen adsorption at the BBD, the DB, and the OD site. The Si—O bond lengths  $d_{\text{Si-O}}$ , the bond angle of the oxygen  $\theta_{\text{Si-O-Si}}$ , the dimer bond lengths  $d_i$ , and the tiltings  $\phi_i$  are tabulated. Here, the tilting of the dimer is represented by the angle between the bond and the  $[1\bar{1}0]$  direction. The suffix  $i=1$  ( $i=2$ ) indicates the reacted (unreacted) dimer. The sums of the bond angles around the up (down) atoms,  $\xi_{1u}$  ( $\xi_{1d}$ ), are also listed. The values of  $d_i$ ,  $\phi_i$ , and  $\xi_{i,u,d}$  on the clean surface are compared. At last, the surface energy is given as relative to the one of the BBD site.

	BBD	DB	OD	Si(001)
$d_{\text{Si-O}}$ (Å)	1.62, 1.67	1.68, 1.59	1.68, 1.71	
$\theta_{\text{Si-O-Si}}$	117°	155°	83°	
$d_1$ (Å)	2.31		2.25	2.32
$\phi_1$	15.8°		1.4°	18.1°
$\xi_{1u}$	278°	292°	360°	285°
$\xi_{1d}$	360°	348°	359°	356°
$d_2$ (Å)	2.32	2.32	2.31	2.32
$\phi_2$	18.3°	18.4°	18.9°	17.3°
$\xi_{2u}$	278°	286°	276°	286°
$\xi_{2d}$	357°	358°	358°	356°
Energy (eV/surface)	0.	0.10	0.23	

bonds and the backbonds. In Table I, the values of  $d_i$ ,  $\phi_i$ , and  $\xi_{i,u,d}$  on the clean surface are compared. Here, we can see that the unreacted dimers are almost unchanged in geometry. As in our previous study,<sup>12</sup> the most energetically stable is the BBD site. The surface energy of the adsorption is listed as relative to the one at the BBD site. Since the differences are not so large, all the adsorption sites are likely to participate in actual oxidation.

Now, we would like to stress that at the BBD site the Si—O bond lengths and the bond angle in Table I are in best agreement with the values obtained in the surface-extended x-ray-absorption fine structure (SEXAFS) and high-

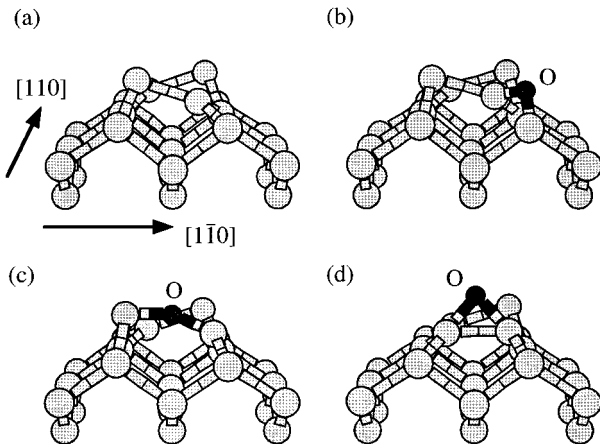


FIG. 1. Perspective views of (a) the Si(001) surface and (b)–(d) the oxygen adsorption at the BBD, the DB, and the OD site, respectively. The oxygen atoms are indicated by the closed circles.

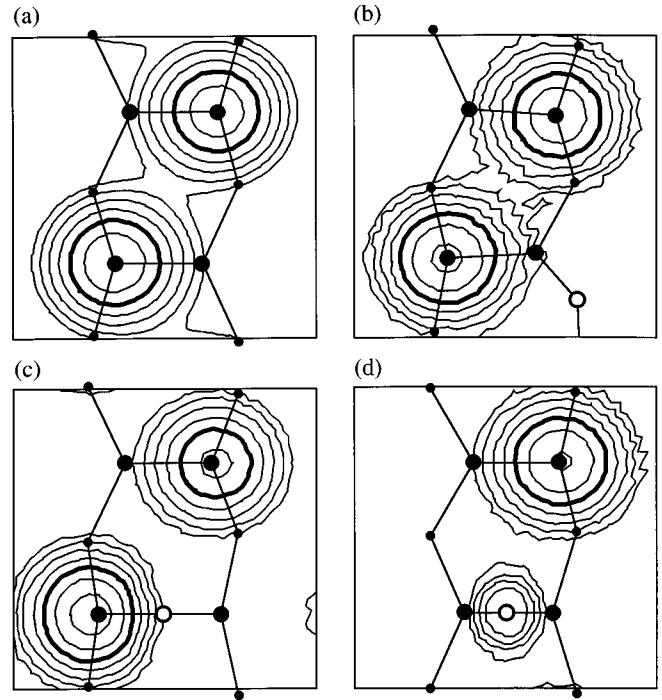


FIG. 2. STM images of (a) the Si(001) surface and (b)–(d) the oxygen adsorption at the BBD, the DB, and the OD site, respectively. The surface bias voltage is taken to be  $V_S = -2$  V (filled-states images). Here, we plot contour maps of the tunneling current on the plane of  $2.4$  Å height from the clean surface. The values of the highest contour (the brightest) are (a)  $5.53 \times 10^{-4}$  and (b)–(d)  $8.25 \times 10^{-4}$  in units of  $e/(\text{a.u.})^3$ . The subsequent ones differ by a factor of 1.49. The thick lines indicate the same value of the current. The jagged lines are artificial in the computational interpolation. The horizontal positions of the O and Si atoms in the outer two layers are denoted by the open and closed circles, respectively.

resolution electron-energy-loss spectroscopy (HREELS) studies<sup>1,4</sup> ( $d_{\text{Si-O}} = 1.65$  Å and  $\theta_{\text{Si-O-Si}} = 120^\circ$  or  $130^\circ$ ). The adsorbed dimer geometry is very similar to that of the clean surface.<sup>12</sup> More interesting is that the Si-O-Si complex at the DB site buckles so as to mimic the original dimer. Then, the up (down) Si atom has a  $p^3$  ( $sp^2$ ) character in the bond configuration:  $\xi_{1u} \sim 270^\circ$  and  $\xi_{1d} \sim 360^\circ$  in Table I. This geometry is expected to induce a charge transfer from the down to the up atom as in the original dimer. These characteristics at the DB site have not been obtained in our previous calculation using the  $p(2 \times 1)$  unit cell. The reason is probably that the second-layer atoms were not relaxed in the dimer-row direction. At the OD site, the oxygen is adsorbed without breaking the dimer although it is nearly symmetric. The oxygen positions about  $0.7$  Å higher than the Si atoms. Here, each dimer atom shows a strong  $sp^2$  character in the bond configuration; the angles of the Si—O bond and the backbonds total  $\xi_{1u,1d} \approx 360^\circ$ . Moreover, the oxygen bond angle is much smaller than the values in crystalline silica. As a result, the remaining  $2p$  orbitals form the dimer bond of a  $\pi$ -bonding character. Bu and Rabalais<sup>2</sup> have argued that the oxygen adsorbs at a site of  $0.5$  Å above the first-layer Si atoms. It might be assigned to the OD site, but not to the DB one.

In Fig. 2, the filled-states STM images of the Si(001)

surface and the oxygen adsorption are shown. The surface bias voltage is taken to be  $V_S = -2$  V, and the scanning plane of the tip is at a height of about 2.4 Å from the surface. Here, we plot contour maps of the tunneling current in the logarithmic scale. The thick lines have the same value of the current in all the figures. The positions of the oxygen and the Si atoms in the outer two layers are indicated by the open and closed circles, respectively.

On the Si(001) surface, the up dimer atoms are observed as bright spots in Fig. 2(a). They give a zigzag line of the dimer row in the STM image. The oxygen adsorption at the BBD and the DB site does not qualitatively affect it; the images shown in Figs. 2(b) and 2(c) are very similar to that of the clean surface. In the figures, however, we should note that the up atoms of the reacted dimers get slightly brighter than the unreacted ones. These atoms should be observed as small protrusions on the surface as in the STM images of Kliese *et al.*<sup>7</sup> This brightness comes from the following two geometrical and electrical reasons. First, the reacted up atoms are slightly lifted by about 0.1 Å. The tunneling current of STM is highly sensitive to the height variance. Second, there arises a charge transfer from the paired down atoms. At the BBD site, the transfer between the dimer atoms is enhanced due to the electronegativity of the oxygen.<sup>11,12</sup> It increases the local density of states (LDOS) on the up atom just below the Fermi level. This electrical effect also enhances the tunneling current. At the DB site, we can expect a charge transfer similar to the one mentioned above. Only for the adsorption at the OD site in Fig. 2(d) is the oxygen atom directly observed as a dull spot. This is a result of the geometry that the oxygen positions fairly high. Because the oxygen  $2p$  orbitals contributing to the current are compact, the spot is expected to rapidly get darker with the STM tip going away from the surface.

Last, we reverse the bias polarity of the tip for the empty-states images. At positive  $V_S = +2$  V, the STM images of the oxygen adsorption drastically change in Fig. 3. Here, the convention is the same as in Fig. 2. In Fig. 3(a) of the clean surface, the dull spots of the down dimer atoms come out in addition to the bright ones. In the adsorption at the BBD site, the dull spot of the adsorbed atom is displaced by about 1 Å in the dimer-row direction as in Fig. 3(b). This displacement is much larger than the geometrical one of the atom (0.2 Å). This feature is due to the tilted dangling bond of the adsorbed down atom, as indicated in Ref. 12. The unreacted dimer twists too slightly to resolve in STM. In Fig. 3(c) for the DB site, the Si-O-Si complex gives a very bright spot of the up atom and a dull spot of the down one. Their distance is about 4 Å, which is widened by about 1 Å compared with that of the unreacted dimer. In the adsorption at the OD site, the reacted dimer is observed dimly on the whole in Fig. 3(d). This is due to the antibonding  $\pi^*$  state of the dimer and the lone-pair orbital of the oxygen. In this way, the empty-states images are characteristic of the oxide geometries. Hence STM observation at positive surface bias is very useful for studying the oxygen adsorption on the Si(001) surface.

### III. SUMMARY

In conclusion, we reinvestigated the oxygen adsorption on the Si(001) surface and the STM images. The adsorbed oxy-

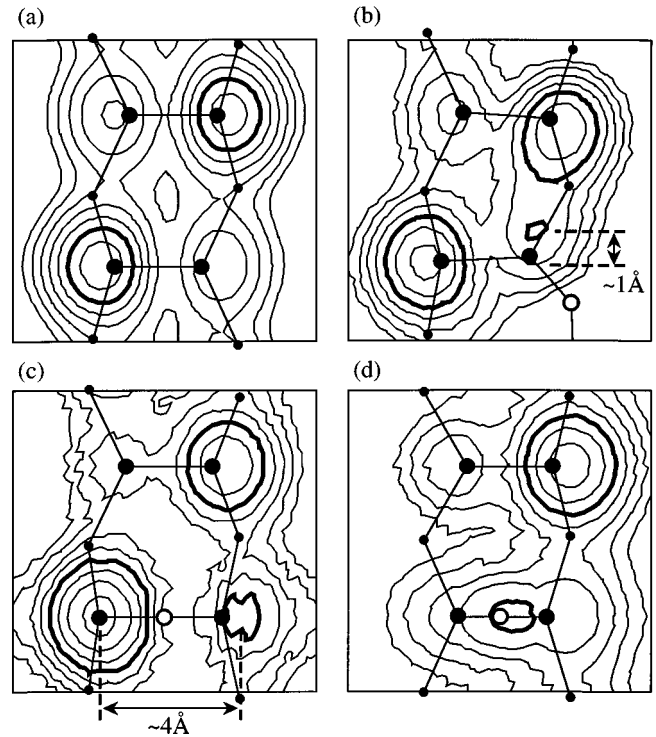


FIG. 3. STM images of (a) the Si(001) surface and (b)–(d) the oxygen adsorption at the BBD, the DB, and the OD site, respectively. The convention is the same as in Fig. 2, but the surface bias voltage is taken to be  $V_S = +2$  V (empty-states images). The values of the highest contour (the brightest) are (a),(b),(d)  $3.35 \times 10^{-4}$ , and (c)  $4.44 \times 10^{-4}$  in units of  $e/(a.u.)^3$ . The subsequent lines differ by a factor of 1.32.

gen gives an atomic structure characteristic of the adsorption site. In particular, we find that the Si-O-S complex at the DB site buckles so as to mimic the original dimer. In the filled-states STM images, the adsorption at the BBD and the DB site appear very similar and almost indistinguishable. There, small protrusions should appear on the surface. This expected feature seems well compatible with the observed one.<sup>7</sup> In the empty-states images, we can find the displaced dull spot of the down dimer atom at the BBD site and the widely separated spots of the original dimer atoms at the DB site. Hence STM observation at the positive bias polarity is indispensable in studying the oxygen adsorption.

Finally, we address an interesting problem on the flip-flop motion of dimers on the Si(001) surface. Wolkow<sup>19</sup> has revealed that at room temperature dimers rapidly switch their buckling orientation. Around atomic defects, however, the buckling is stabilized and the asymmetric dimers are observed.<sup>19,20</sup> This is likely the case for the adsorption at the BBD site because of the strong asymmetry and the energetic stability. Actually, stabilized dimer buckling around the small protrusions have been observed in the STM images.<sup>7,8</sup> How would the dynamics of the dimers be around the oxygen at the DB and the OD site? If the Si-O-Si complex at the DB site can easily change the buckling orientation along with the surrounding dimers, it will appear symmetric in the STM images of Figs. 2(c) and 3(c).

## ACKNOWLEDGMENTS

We are very thankful to Dr. J. Yamauchi and Dr. S. Watanabe for their kind support to the numerical computations,

which were carried out at the Computer Center of University of Tokyo. In Fig. 1, we used XMOL, version 1.3.1, developed at Minnesota Supercomputer Center, Inc., Minneapolis MN, 1993.

- 
- <sup>1</sup>L. Incoccia, A. Balerna, S. Cramm, C. Kunz, F. Senf, and I. Storzjohann, *Surf. Sci.* **189/190**, 453 (1987).
  - <sup>2</sup>H. Bu and J.W. Rabalais, *Surf. Sci.* **301**, 285 (1994).
  - <sup>3</sup>H. Ibach, H.D. Bruchmann, and H. Wagner, *Appl. Phys. A* **29**, 113 (1982).
  - <sup>4</sup>J.A. Schaefer, F. Stucki, D.J. Frankel, W. Göpel, and G.L. Lapeyre, *J. Vac. Sci. Technol. B* **2**, 359 (1984); J.A. Schaefer and W. Göpel, *Surf. Sci.* **155**, 535 (1985).
  - <sup>5</sup>H. Ikegami, K. Ohmori, H. Ikeda, H. Iwano, S. Zaima, and Y. Yasuda, *Jpn. J. Appl. Phys.* **35**, 1593 (1996).
  - <sup>6</sup>J.R. Engstrom, D.J. Bonser, and T. Engel, *Surf. Sci.* **268**, 238 (1992).
  - <sup>7</sup>P. Kliese, B. Röttger, D. Badt, and H. Neddermeyer, *Ultramicroscopy* **42-44**, 824 (1992).
  - <sup>8</sup>Ph. Avouris and D.G. Cahill, *Ultramicroscopy* **42-44**, 838 (1992); D.G. Cahill and Ph. Avouris, *Appl. Phys. Lett.* **60**, 326 (1992).
  - <sup>9</sup>M. Udagawa, Y. Umetani, H. Tanaka, M. Itoh, T. Uchiyama, Y. Watanabe, T. Yokotsuka, and I. Sumita, *Ultramicroscopy* **42-44**, 946 (1992).
  - <sup>10</sup>Y. Miyamoto and A. Oshiyama, *Phys. Rev. B* **41**, 12 680 (1990); Y. Miyamoto, A. Oshiyama, and A. Ishitani, *Solid State Commun.* **74**, 343 (1990).
  - <sup>11</sup>Y. Miyamoto, *Phys. Rev. B* **46**, 12 473 (1992).
  - <sup>12</sup>T. Uchiyama and M. Tsukada, *Phys. Rev. B* **53**, 7917 (1996); *Surf. Sci.* **357/358**, 509 (1996).
  - <sup>13</sup>K. Laasonen, A. Pasquarello, R. Car, C. Lee, and D. Vanderbilt, *Phys. Rev. B* **47**, 10 142 (1993).
  - <sup>14</sup>J. Yamauchi, M. Tsukada, S. Watanabe, and O. Sugino, *Surf. Sci.* **341**, L1037 (1995); *Phys. Rev. B* **54**, 5586 (1996).
  - <sup>15</sup>D. Vanderbilt, *Phys. Rev. B* **41**, 7892 (1990).
  - <sup>16</sup>A. Ramstad, G. Brocks, and P.J. Kelly, *Phys. Rev. B* **51**, 14 504 (1995).
  - <sup>17</sup>J. Fritsch and P. Pavone, *Surf. Sci.* **344**, 159 (1995).
  - <sup>18</sup>R.W.G. Wyckoff, *Crystal Structures*, 2nd ed. (Interscience, New York, 1965).
  - <sup>19</sup>R.A. Wolkow, *Phys. Rev. Lett.* **68**, 2636 (1992).
  - <sup>20</sup>H. Tochiyama, T. Amakusa, and M. Iwatsuki, *Phys. Rev. B* **50**, 12 262 (1994).